Published in final edited form as:
J Am Chem Soc. 2019 June 05; 141(22): 8737–8740. doi:10.1021/jacs.9b03766.

Postsynthetic Metalation of a Robust Hydrogen-Bonded Organic Framework for Heterogeneous Catalysis

Bin Han[†], **Hailong Wang**[*,†], **Chiming Wang**[†], **Hui Wu**[§], **Wei Zhou**[§], **Banglin Chen**[*,‡], **Jianzhuang Jiang**[*,†]

[†] Beijing Key Laboratory for Science and Application of Functional Molecular and Crystalline Materials, Department of Chemistry, University of Science and Technology Beijing, Beijing 100083, China

[‡] Department of Chemistry, University of Texas at San Antonio, San Antonio, Texas 78249-0698, United States

[§] Center for Neutron Research, National Institute of Standards and Technology, Gaithersburg, Maryland 20899-6102, United States

Abstract

Hydrogen-bonded organic framework (HOF)-based catalysts still remain unreported thus far due to their relatively weak stability. In the present work, a robust porous HOF (HOF-19) with a Brunauer–Emmett–Teller surface area of 685 m^2 g^{-1} was reticulated from a cagelike building block, amino-substituted bis(tetraoxacalix[2]arene[2]triazine), depending on the hydrogen bonding with the help of $\pi-\pi$ interactions. The postsynthetic metalation of HOF-19 with palladium acetate afforded a palladium(II)-containing heterogeneous catalyst with porous hydrogen-bonded structure retained, which exhibits excellent catalytic performance for the Suzuki–Miyaura coupling reaction with the high isolation yields (96−98%), prominent stability, and good selectivity. More importantly, by simple recrystallization, the catalytic activity of deactivated species can be recovered from the isolation yield 46% to 92% for 4-bromobenzonitrile conversion at the same conditions, revealing the great application potentials of HOF-based catalysts.

Heterogeneous catalysis plays a dominant role in the chemical and pharmaceutical industry.[1] As a result, continuous efforts have been paid toward developing effective methods for synthesizing heterogeneous catalysts with high efficiency and in particular with an easy recovery and recycling nature. In the past several years, by immobilizing homogeneous catalysts inside the porous supports such as zeolites,[2] metal–organic frameworks (MOFs),[3] and covalent organic frameworks (COFs),[4] diverse heterogeneous catalysts with boosted

---

[*] **Corresponding Authors** hlwang@ustb.edu.cn, banglin.chen@utsa.edu, jianzhaung@ustb.edu.cn.

ASSOCIATED CONTENT

Supporting Information

The Supporting Information is available free of charge on the ACS Publications website at DOI: 10.1021/jacs.9b03766.

Experimental details, NMR spectra, TGA curve, SEM photos, PXRD patterns, XPS spectra, EDS mapping of HOF-19 and/or HOF-19⊃Pd(II) (PDF) Crystallographic data for HOF-19 (CIF)

The authors declare no competing financial interest.

activity and stability have been fabricated. However, the regeneration of these heterogeneous catalysts is still challenging due to their nonrenewable porous supports.

In the same way as MOFs and COFs, porous hydrogen-bonded organic frameworks (HOFs) are self-assembled from discrete molecular modules as well.[5] Despite the outstanding properties of HOFs revealed in the fields of gas storage,[6] small-molecule separation,[7] sensing,[8] and proton conduction,[9] reports over HOF-based catalysts still remain unknown, to the best of our knowledge, due to the relatively poor stability associated with the weak hydrogen bonding connection between discrete building blocks in HOFs.[5–9] Fortunately, the introduction of additional $\pi-\pi$ interactions would significantly enhance the stability when aromatic building blocks are employed for constructing HOFs,[5g,6f] rendering it possible to fabricate heterogeneous catalysts with robust frameworks as the porous support of homogeneous species. In particular, the excellent recyclability of HOFs through simple recrystallization enables them to be regenerated easily, thus endowing the sustainable advantage to HOF-based catalysts.

Herein, a novel organic cage of amino-substituted bis(tetraoxacalix[2]arene[2]triazine) (**L**) composed of five six-membered aromatic rings has been designed and prepared as a building block for assembling HOFs (Figure 1a and Scheme S1, Supporting Information). Depending on the hydrogen bonding between neighboring building blocks with the help of rich $\pi-\pi$ interactions between intercage aromatic moieties, the first cage-based HOF (HOF-19) is constructed, and its hydrogen-bonded structure is clearly revealed by single-crystal X-ray diffraction analysis. The N_2 sorption measurement at 77 K discloses a Brunauer–Emmett–Teller (BET) surface area of 685 $m^2 g^{-1}$ for activated HOF-19. Postfunctionalization of this HOF with palladium acetate gives a palladium(II)-containing HOF-19⊃Pd(II) with parent hydrogen-bonded structure maintained according to the powder X-ray diffraction (PXRD) analysis, indicating the robustness of HOF-19. Further evidence on the robustness of HOF-19 comes from the excellent stability and recyclability of HOF-19⊃Pd(II) in *p*-xylene in the presence of potassium carbonate at 150 °C. Under such experimental conditions, the Suzuki–Miyaura coupling reaction is able to be selectively promoted in high isolation yields (96−98%), revealing the predominant catalytic activity of HOF-based materials for the first time. Nevertheless, the catalytic activity of deactivated species, with the 46% isolation yield for the conversion of 4-bromobenzonitrile, is recovered to 92% by simple recrystallization regeneration, revealing the great application potentials of HOF-based catalysts.

A facile reaction between chloride-substituted bis(tetraoxacalix[2]arene[2]triazine)[10] and ammonium hydroxide afforded **L** (Scheme S1 and Figures S1 and S2, Supporting Information). The slow evaporation of the formic acid solution of **L** gave single crystals of HOF-19 with poor solubility in common organic solvents (except only DMSO). Single-crystal X-ray diffraction data confirms the three-dimensional (3D) porous structure of HOF-19 (Figure 1; Tables S1 and S2, Supporting Information). As exhibited in Figure 1, depending on the multiple N−H···N hydrogen bonding between intercage 2-aminotriazinyl (AT) groups with the help of $\pi-\pi$ interactions from intercage benzene moieties, two-dimensional porous hydrogen-bonded supramolecular structures containing one-dimensional (1D) channels with the size of 8.0 × 13.6 Å along the [010] direction are formed, which are further packed into the 3D architecture of HOF-19 depending on the intercage cofacial $\pi-\pi$

interaction between AT groups and C−H⋯π interaction (actually a kind of $\pi-\pi$ interaction). The PLATON calculation discloses 47% void space for HOF-19,[11] which should be favorable for the molecular substrate diffusion.

The bulk material of HOF-19 with good thermal stability was obtained by diffusing acetone into the formic acid solution of **L** (Figure S3, Supporting Information). Acetone-exchanged HOF-19 was degassed at 25 °C to give an activated sample (HOF-19a). The PXRD pattern of HOF-19a is well consistent with the simulated profile of HOF-19 (Figures S4 and S5, Supporting Information), indicating its robust nature. The N_2 sorption measurement at 77 K reveals its type I adsorption curve with a N_2 uptake of 287 $cm^3 g^{-1}$ at 1.0 bar (Figure 2). The experimental pore volume of 0.45 $cm^3 g^{-1}$ is well consistent with the theoretical value (0.48 $cm^3 g^{-1}$; Table S1).[11] The BET surface area of HOF-19a was calculated to be 685 $m^2 g^{-1}$.

The multiple hydrogen bonding and $\pi-\pi$ interactions between neighboring cages enhance the robustness of HOF-19. The poor solubility of HOF-19 in common organic solvents could effectively stabilize the framework in solution. In addition, abundant triazinyl nitrogen atoms and amino groups inside the pores of HOF-19 provide enough binding sites to incorporate catalytically active metal ions. All these characteristics inspire us to fabricate a heterogeneous catalyst with HOF-19 as the porous support. The immersion of activated HOF in an acetone solution of palladium acetate (0.100 mM) afforded palladium(II)-containing HOF-19⊐Pd(II). Its PXRD pattern matches well with the simulated one for HOF-19 in Figure S6 (Supporting Information), indicating the hydrogen-bonded structure retained by the post-treated species and illustrating the HOF robustness again. Inductively coupled plasma (ICP) analysis gives a Pd content of 3.8 wt % included in HOF-19⊐Pd(II). In the X-ray photoelectron spectrum shown in Figure S7 (Supporting Information), the observation of two peaks with the binding energy of 338.1 and 343.4 eV corresponding to Pd $3d_{5/2}$ and Pd $3d_{3/2}$, respectively, confirms divalent palladium ions bound by HOF-19. The slight downshift of Pd $3d_{5/2}$ and Pd $3d_{3/2}$ binding energy for HOF-19⊐Pd(II) relative to that (338.3 and 343.6 eV) of palladium acetate indicates the presence of an interaction between Pd^{2+} ions and HOF-19.[12] The slight upshift for the binding energy of the amino group of HOF-19 after including palladium acetate not only indicates HOF-19 interacting with Pd^{2+} ions but also suggests the amino groups, instead of the intracage cavity, as active sites to bind the metal ions (Figure S8, Supporting Information). The energy-dispersive spectroscopy (EDS) mapping of HOF-19⊐Pd(II) clearly hints at the homogeneous distribution of the Pd element, excluding the presence of Pd nanoparticles (Figure S9, Supporting Information). After postmodification with $Pd(OAc)_2$ to give HOF-19⊐Pd(II) with palladium ions decorated on the surface of HOF channels, the BET surface area was decreased to 159 $m^2 g^{-1}$, indicating the partial structural collapse of HOF after Pd^{2+} inclusion.

To illustrate the proof-of-concept of the HOF-based catalyst, the Suzuki–Miyaura coupling reaction was selected as a model reaction to examine the catalytic activity of HOF-19⊐Pd(II). As can be found in Table 1, in the presence of 0.260 mmol % HOF-19⊐Pd(II), the halogenated benzene substrates (entries 1–6) were successfully transformed to corresponding coupling products in the high isolation yields of 96–98% within a short time of 1.5–2.5 h. In particular, for the conversion of 1-bromo-4-nitrobenzene, only about 0.260% Pd content in HOF-19⊐Pd(II) was revealed to be leached into the filtrate according to the ICP measurement, indicating the strong interaction between Pd^{2+} and HOF-19. Under the same conditions, the catalytic activity of 0.260 mmol % HOF-19⊃Pd(II) is even comparable to the excellent performance of 0.500 mmol % COF-LZU1⊃Pd(II) catalyst toward the reaction of 1-bromo-4-methoxybenzene with phenylboronic acid,[12] indicating the excellent catalytic activity of HOF-19⊃Pd(II) (Table 1). Nevertheless, HOF-19⊃Pd(II) shows a much higher catalytic efficiency in comparison with palladium acetate, a mixture of HOF-19 and palladium acetate, and Pd/C catalyst, confirming the crucial role of palladium(II) ions deposited on the channel surfaces of HOF-19 on the present heterogeneous catalysis of the Suzuki–Miyaura coupling reaction. Interestingly, under the same reaction conditions, the substrates of 4′-bromo-1,1′-biphenyl and 4-methoxy-4′-bromo-1,1′-biphenyl with large molecular size of 7.5 × 13.9 and 7.5 × 16.0 Å, respectively, were converted into the corresponding product only with the isolation yield below 20% even after 4.0 h, which are even much lower than those with $Pd(OAc)_2$ as the catalyst (Table 1 and Table S3, Supporting Information), indicating the presence of pore size selectivity of the HOF-19⊃Pd(II) catalyst.

The recyclability of HOF-19⊃Pd(II) catalyst was evaluated in the conversion of 4-bromobenzonitrile. HOF-19⊃Pd(II) kept an almost constant catalytic activity and good crystallinity for four cycles of reaction, indicating again the good stability of the HOF-based catalyst (Figures S6 and S10, Supporting Information). The isolated yield for the fifth reaction cycle was reduced to ca. 74%. After the continuous coupling reaction of 4-bromobenzonitrile for 20.0 h, HOF-19⊃Pd(II) was deactivated with the low isolation yield of 46%. However, recrystallization of deactivated catalyst afforded a regenerated crystalline sample (Figure S11, Supporting Information). More importantly, this regenerated catalyst displayed a recovered catalytic activity toward 4-bromobenzonitrile with the 92% isolation yield (Figure S12, Supporting Information), revealing the sustainable advantage of this newly developed HOF-based catalyst.

In summary, a novel cage-based HOF with permanent porosity has been synthesized for the first time. Multiple hydrogen bonding interactions together with the $\pi-\pi$ interactions enhance the stability of HOF. With this porous HOF as a robust support of palladium acetate, a highly efficient and selective HOF-based heterogeneous catalyst has been realized toward the Suzuki–Miyaura coupling reaction. In particular, by utilizing the recycling advantage of HOFs, this HOF-based catalyst could be easily regenerated through simple recrystallization, exhibiting almost recovered activity. These results reveal the great application potentials of HOF-based catalysts. We hope the present result will ignite more research interest toward exploration of HOF-based catalysts and other applications.

Supplementary Material

Refer to Web version on PubMed Central for supplementary material.

ACKNOWLEDGMENTS

Financial support from the Natural Science Foundation of China (21631003 and 21805005), the Fundamental Research Funds for the Central Universities (FRF-BD-17-016A), Welch Foundation (AX-1730), National Science Foundation (DMR-1606826), and University of Science and Technology Beijing is gratefully acknowledged.

REFERENCES

(1). Deutschmann O; Knözinger H; Kochloefl K; Turek T. Heterogeneous Catalysis and Solid Catalysts, Fundamentals. In Ullmann's Encyclopedia of Industrial Chemistry; Wiley-VCH Verlag GmbH & Co. KGaA, 2000.

(2) (a). Dusselier M; Davis ME Small-Pore Zeolites: Synthesis and Catalysis. Chem. Rev 2018, 118, 5265. [PubMed: 29746122] (b)Wang N; Sun Q; Bai R; Li X; Guo G; Yu J. In Situ Confinement of Ultrasmall Pd Clusters within Nanosized Silicalite-1 Zeolite for Highly Efficient Catalysis of Hydrogen Generation. J. Am. Chem. Soc 2016, 138, 7484. [PubMed: 27248462]

(3) (a). Furukawa H; Cordova KE; O'Keeffe M; Yaghi OM The Chemistry and Applications of Metal–Organic Frameworks. Science 2013, 341, 974.(b)Xiao J-D; Jiang H-L Metal–Organic Frameworks for Photocatalysis and Photothermal Catalysis. Acc. Chem. Res 2019, 52, 356. [PubMed: 30571078] (c)Bai Y; Dou Y; Xie L-H; Rutledge W; Li J-R; Zhou H-C Zr-Based Metal–Organic Frameworks: Design, Synthesis, Structure, and Applications. Chem. Soc. Rev 2016, 45, 2327. [PubMed: 26886869] (d)Zhu Q-L; Xu Q. Metal–Organic Framework Composites. Chem. Soc. Rev 2014, 43, 5468. [PubMed: 24638055] (e)Li B; Wen H-M; Cui Y; Zhou W; Qian G; Chen B. Emerging Multifunctional Metal–Organic Framework Materials. Adv. Mater 2016, 28, 8819. [PubMed: 27454668] (f)Drake T; Ji P; Lin W. Site Isolation in Metal–Organic Frameworks Enables Novel Transition Metal Catalysis. Acc. Chem. Res 2018, 51, 2129. [PubMed: 30129753] (g)Evans JD; Sumbya CJ; Doonan CJ Post-Synthetic Metalation of Metal–Organic Frameworks. Chem. Soc. Rev 2014, 43, 5933. [PubMed: 24736674] (h)Cohen SM Postsynthetic Methods for the Functionalization of Metal–Organic Frameworks. Chem. Rev 2012, 112, 970. [PubMed: 21916418] (i)Bloch ED; Britt D; Lee C; Doonan CJ; Fernando JU-R; Furukawa H; Long JR; Yaghi OM Metal Insertion in a Microporous Metal–Organic Framework Lined with 2,2'-Bipyridine. J. Am. Chem. Soc 2010, 132, 14382. [PubMed: 20849109] (j)Niu Z; Gunatilleke WDCB; Sun Q; Lan PC; Perman J; Ma J-G; Cheng Y; Aguila B; Ma S. Metal–Organic Framework Anchored with a Lewis Pair as a New Paradigm for Catalysis. Chem. 2018, 4, 2587.(k)Liu J; Ye J; Li Z; Otake K-I; Liao Y; Peters AW; Noh H; Truhlar DG; Gagliardi L; Cramer CJ; Farha OK; Hupp JT Beyond the Active Site: Tuning the Activity and Selectivity of a Metal–Organic Framework-Supported Ni Catalyst for Ethylene Dimerization. J. Am. Chem. Soc 2018, 140, 11174. [PubMed: 30141922] (l)Liao P-Q; Shen J-Q; Zhan J-P Metal–Organic Frameworks for Electrocatalysis. Coord. Chem. Rev 2018, 373, 22.(m)He W-L; Zhao M; Wu C-D A Versatile Metalloporphyrinic Framework Platform for Highly Efficient Bioinspired, Photo- and Asymmetric Catalysis. Angew. Chem., Int. Ed 2019, 58, 168.

(4) (a). Lin S; Diercks CS; Zhang Y-B; Kornienko N; Nichols EM; Zhao Y; Paris AR; Kim D; Yang P; Yaghi OM; Chang CJ Covalent Organic Frameworks Comprising Cobalt Porphyrins for Catalytic CO2 Reduction in Water COF. Science 2015, 349, 1208. [PubMed: 26292706] (b)Lu S; Hu Y; Wan S; McCaffrey R; Jin Y; Gu H; Zhang W. Synthesis of Ultrafine and Highly Dispersed Metal Nanoparticles Confined in a Thioether-Containing Covalent Organic Framework and Their Catalytic Applications. J. Am. Chem. Soc 2017, 139, 17082. [PubMed: 29095604]

(5) (a). Barrer RM; Shanson VH Dianin's Compound as a Zeolitic Sorbent. J. Chem. Soc., Chem. Commun 1976, 9, 333.(b)Lee F; Gabe E; Tse JS; Ripmeester JA Crystal Structure, CP/MAS 129Xe, and 13C NMR of Local Ordering in Dianin's Compound Clathrates. J. Am. Chem. Soc 1988, 110, 6014. [PubMed: 22148775] (c)Lloyd GO; Bredenkamp MW; Barbour LJ Enclathration of Morpholinium Cations by Dianin's Compound: Salt Formation by Partial Host-to-Guest Proton Transfer. Chem. Commun 2005, 4053.(d)Simard M; Su D; Wuest JD Use of Hydrogen Bonds to Control Molecular Aggregation. Self-Assembly of Three-Dimensional Networks with Large Chambers. J. Am. Chem. Soc 1991, 113, 4696.(e)McKeown NB Nanoporous Molecular Crystals. J. Mater. Chem 2010, 20, 10588.(f)Adachi T; Ward MD Versatile and Resilient Hydrogen-Bonded Host Frameworks. Acc. Chem. Res 2016, 49, 2669. [PubMed: 27689535] (g)Lin R; He Y; Li P; Wang H; Zhou W; Chen B. Multifunctional Porous Hydrogen-Bonded Organic Framework Materials. Chem. Soc. Rev 2019, 48, 1362. [PubMed: 30676603] (h)Brunet P; Simard M; Wuest JD Molecular Tectonics. Porous Hydrogen-Bonded Networks with Unprecedented Structural Integrity. J. Am. Chem. Soc 1997, 119, 2737.(i)Luo J; Wang J-W; Zhang J-H; Lai S; Zhong D-C Hydrogen-Bonded Organic Frameworks: Design, Structures and Potential Applications. CrystEngComm 2018, 20, 5884.(j)Endo K; Sawaki T;

Koyanagi M; Kobayashi K; Masuda H; Aoyama Y. Guest-Binding Properties of Organic Crystals Having an Extensive Hydrogen-Bonded Network: An Orthogonal Anthracene-Bis-(resorcino1) Derivative as a Functional Organic Analog of Zeolites. J. Am. Chem. Soc 1995, 117, 8341. (k)Saied O; Maris T; Wuest JD Deformation of Porous Molecular Networks Induced by the Exchange of Guests in Single Crystals. J. Am. Chem. Soc 2003, 125, 14956. [PubMed: 14653708] (l)Kobayashi K; Sato A; Sakamoto S; Yamaguchi K. Solvent-Induced Polymorphism of Three-Dimensional Hydrogen-Bonded Networks of Hexakis(4-carbamoylphenyl)benzene. J. Am. Chem. Soc 2003, 125, 3035. [PubMed: 12617670] (m)Liu Y; Hu C; Comotti A; Ward MD Supramolecular Archimedean Cages Assembled with 72 Hydrogen Bonds. Science 2011, 333, 436. [PubMed: 21778396] (n)Soldatov DV; Moudrakovski IL; Grachev EV; Ripmeester JA Micropores in Crystalline Dipeptides as Seen from the Crystal Structure, He Pycnometry, and 129Xe NMR Spectroscopy. J. Am. Chem. Soc 2006, 128, 6737. [PubMed: 16704277] (o)Tian J; Thallapally PK; Dalgarno SJ; Atwood JL Free Transport of Water and CO2 in Nonporous Hydrophobic Clarithromycin Form II Crystals. J. Am. Chem. Soc 2009, 131, 13216. [PubMed: 19715295]

(6) (a). Dalrymple SA; Shimizu GKH Crystal Engineering of a Permanently Porous Network Sustained Exclusively by Charge-Assisted Hydrogen Bonds. J. Am. Chem. Soc 2007, 129, 12114. [PubMed: 17880091] (b)Hisaki I; Nakagawa S; Tohnai N; Miyata M. A C3-Symmetric Macrocycle-Based, Hydrogen-Bonded, Multiporous Hexagonal Network as a Motif of Porous Molecular Crystals. Angew. Chem., Int. Ed 2015, 54, 3008.(c)Hu F; Liu C; Wu M; Pang J; Jiang F; Yuan D; Hong M. An Ultrastable and Easily Regenerated Hydrogen-Bonded Organic Molecular Framework with Permanent Porosity. Angew. Chem., Int. Ed 2017, 56, 2101. (d)Mastalerz M; Oppel IM Rational Construction of an Extrinsic Porous Molecular Crystal with an Extraordinary High Specific Surface Area. Angew. Chem., Int. Ed 2012, 51, 5252.(e)Pulido A; Chen L; Kaczorowski T; Holden D; Little MA; Chong SY; Slater BJ; McMahon DP; Bonillo B; Stackhouse CJ; Stephenson A; Kane CM; Clowes R; Hasell T; Cooper AI; Day GM Functional Materials Discovery Using Energy-Structure-Function Maps. Nature 2017, 543, 657. [PubMed: 28329756] (f)Yin Q; Zhao P; Sa R-J; Chen G-C; Lü J; Liu T-F; Cao R. An Ultra-Robust and Crystalline Redeemable Hydrogen-Bonded Organic Framework for Synergistic Chemo-Photodynamic Therapy. Angew. Chem., Int. Ed 2018, 57, 7691.

(7) (a). Chen T-H; Popov I; Kaveevivitchai W; Chuang Y-C; Chen Y; Daugulis O; Jacobson AJ; Miljanic OS Thermally Robust and Porous Noncovalent Organic Framework with High Affinity for Fluorocarbons and CFCs. Nat. Commun 2014, 5, 5131. [PubMed: 25307413] (b)Luo X-Z; Jia X-J; Deng J-H; Zhong J-L; Liu H-J; Wang KJ; Zhong D-C A Microporous Hydrogen-Bonded Organic Framework: Exceptional Stability and Highly Selective Adsorption of Gas and Liquid. J. Am. Chem. Soc 2013, 135, 11684. [PubMed: 23885835] (c)He Y; Xiang S; Chen B. A Microporous Hydrogen-Bonded Organic Framework for Highly Selective C2H2/C2H4 Separation at Ambient Temperature. J. Am. Chem. Soc 2011, 133, 14570. [PubMed: 21863860] (d)Li P; He Y; Zhao Y; Weng L; Wang H; Krishna R; Wu H; Zhou W; O'Keeffe M; Han Y; Chen B. A Rod-Packing Microporous Hydrogen-Bonded Organic Framework for Highly Selective Separation of C2H2/CO2 at Room Temperature. Angew. Chem., Int. Ed 2014, 54 (2), 574–577. (e)Li P; He Y; Guang J; Weng L; Zhao JC-G; Xiang S; Chen B. A Homochiral Microporous Hydrogen-Bonded Organic Framework for Highly Enantio Selective Separation of Secondary Alcohols. J. Am. Chem. Soc 2014, 136, 547. [PubMed: 24392725] (f)Wang H; Li B; Wu H; Hu T-L; Yao Z; Zhou W; Xiang S; Chen B. A Flexible Microporous Hydrogen-Bonded Organic Framework for Gas Sorption and Separation. J. Am. Chem. Soc 2015, 137, 9963. [PubMed: 26214340] (g)Bao Z; Xie D; Chang G; Wu H; Li L; Zhou W; Wang H; Zhang Z; Xing H; Yang Q; Zaworotko MJ; Ren Q; Chen B. Fine Tuning and Specific Binding Sites with a Porous Hydrogen-Bonded Metal-Complex Framework for Gas Selective Separations. J. Am. Chem. Soc 2018, 140, 4596. [PubMed: 29540058] (h)Zhou D-D; Xu Y-T; Lin R-B; Mo Z-W; Zhang W-X; Zhang J-P High-Symmetry Hydrogen-Bonded Organic Frameworks: Air Separation and Crystal-to-Crystal Structural Transformation. Chem. Commun 2016, 52, 4991.

(8). Hisaki I; Suzuki Y; Gomez E; Ji Q; Tohnai N; Nakamura T; Douhal A. Acid Responsive Hydrogen-Bonded Organic Frameworks. J. Am. Chem. Soc 2019, 141, 2111. [PubMed: 30615836]

(9) (a). Xing G; Yan T; Das S; Ben T; Qiu S. Synthesis of Crystalline Porous Organic Salts with High Proton Conductivity. Angew. Chem., Int. Ed 2018, 57, 5345.(b)Karmakar A; Illathvalappil R;

Anothumakkool B; Sen A; Samanta P; Desai AV; Kurungot S; Ghosh SK Hydrogen-Bonded Organic Frameworks (HOFs): A New Class of Porous Crystalline Proton-Conducting Materials. Angew. Chem., Int. Ed 2016, 55, 10667.

(10). Wang D-X; Wang Q-Q; Han Y; Wang Y; Huang Z-T; Wang M-X Versatile Anion-Interactions between Halides and a Conformationally Rigid Bis(tetraoxacalix[2]arene[2]triazine) Cage and Their Directing Effect on Molecular Assembly. Chem. - Eur. J 2010, 16, 13053. [PubMed: 20967911]

(11). Spek AL PLATON: A Multipurpose Crystallographic Tool; Utrecht University, Utrecht, The Netherlands, 2005.

(12). Ding S-Y; Gao J; Wang Q; Zhang Y; Song W-G; Su C-Y; Wang W. Construction of Covalent Organic Framework for Catalysis: Pd/COF-LZU1 in Suzuki-Miyaura Coupling Reaction. J. Am. Chem. Soc 2011, 133, 19816. [PubMed: 22026454]

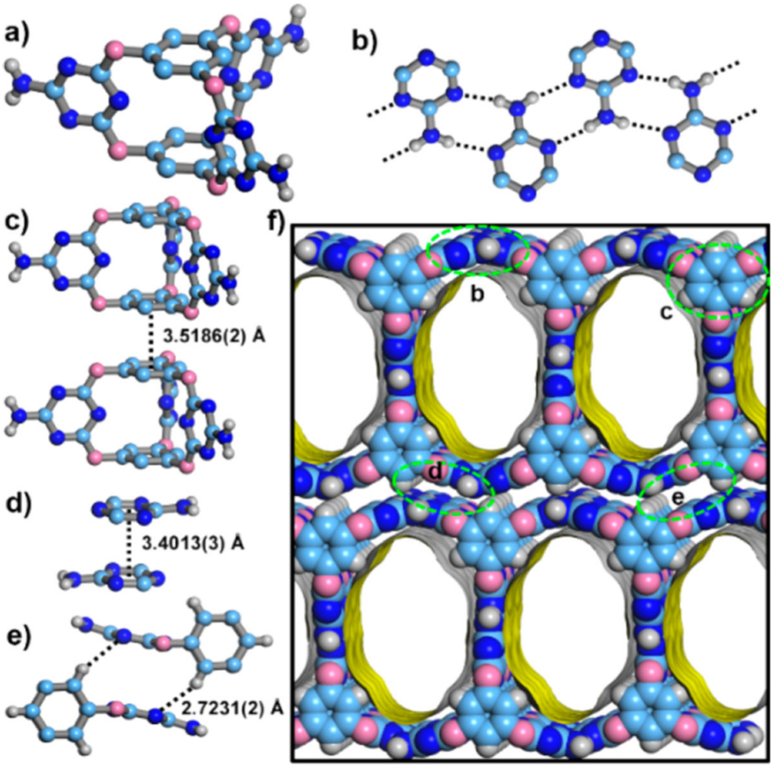

Figure 1.

Crystal structure of HOF-19 showing (a) molecular organic cage **L**; (b) hydrogen bonding ribbon comprising neighboring AT groups; (c, d) two kinds of intercage cofacial $\pi-\pi$ interactions; (e) the C−H···π interaction; and (f) a packing diagram of HOF-19 showing the 1D channel surfaces highlighted as yellow/gray (inner/outer) curved planes (C, slight cyan; O, pink; N, blue; H, white).

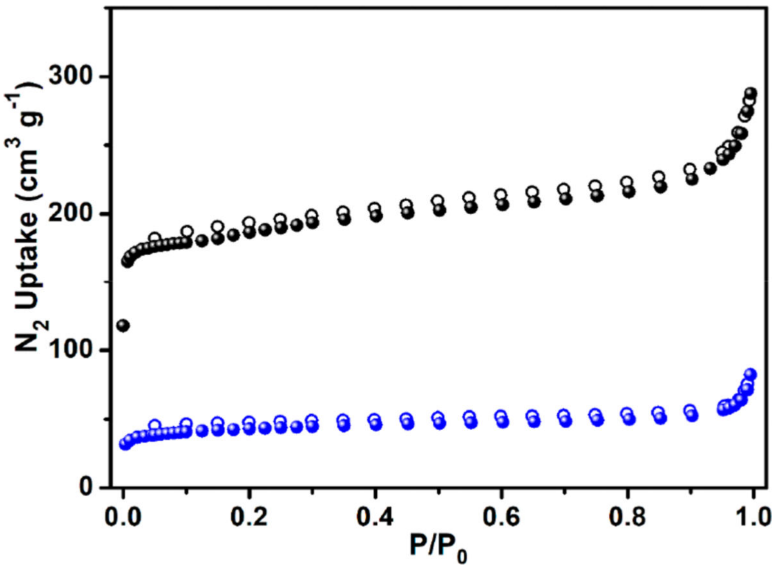

Figure 2.

N_2 sorption isotherms of HOF-19a (black) and HOF-19⊃Pd(II) (blue) at 77 K (solid symbols, adsorption; open symbols, desorption).

Table 1.

Catalytic Performance of HOF-19⊃Pd(II) Catalyst in the Suzuki–Miyaura Coupling Reaction[a]

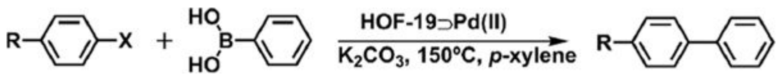

entry	R	X	time (h)	yield[b] (%)
1	−CHO	Br	2.5	97
2	−CN	Br	1.5	97
3	−H	Br	2.0	98
4	−NO2	Br	2.5	97
5	−OMe	Br	2.0	96
6	−OMe	I	1.5	97
7	−Ph	Br	4.0	19
8	−PhOMe	Br	4.0	13
9[c]	−OMe	Br	4.0	96
10[d]	−OMe	Br	4.0	71
11[e]	−OMe	Br	4.0	70
12[f]	−OMe	Br	4.0	~7
13[d]	−Ph	Br	4.0	69
14[d]	−PhOMe	Br	4.0	58

[a] Reaction conditions: aryl halide (1.00 mmol), phenylboronic acid (1.50 mmol), K_2CO_3 (2.00 mmol), HOF-19⊃Pd(II) (7.5 mg, 0.260 mmol %), *p*-xylene (4 mL), 150 °C.

[b] Isolation yield.

[c] 0.500 mmol % COF-LZU1⊃Pd(II).[11]

[d] 0.260 mmol % $Pd(OAc)_2$.

[e] 0.260 mmol % $Pd(OAc)_2$ and HOF-19 (7.5 mg).

[f] 0.260 mmol % Pd/C (10 wt %).